JOURNAL OF VIROLOGY, Oct. 1997, p. 7404–7420 Vol. 71, No. 10
0022-538X/97/$04.00+0

Vaccinia Virus Membrane Proteins p8 and p16 Are Cotranslationally Inserted into the Rough Endoplasmic Reticulum and Retained in the Intermediate Compartment

TESSA SALMONS,[1] ANNETT KUHN,[1] FIONA WYLIE,[1]† SIBYLLE SCHLEICH,[1] JUAN RAMON RODRIGUEZ,[2] DOLORES RODRIGUEZ,[2] MARIANO ESTEBAN,[2] GARETH GRIFFITHS,[1] AND JACOMINE KRIJNSE LOCKER[1]*

European Molecular Biology Laboratory, 69117 Heidelberg, Germany,[1] and Centro Nacional de Biotecnologia, Campus Universidad Autonoma, 28049 Madrid, Spain[2]

Received 31 March 1997/Accepted 15 July 1997

The use of two-dimensional gel electrophoresis has identified the gene products A14L (p16) and A13L (p8) as abundant membrane proteins of the first infectious form of vaccinia virus, the intracellular mature virus (IMV; O. N. Jensen, T. Houthaeve, A. Shevchenko, S. Cudmore, T. Ashford, M. Mann, G. Griffiths, J. Krijnse Locker, J. Virol. 70:7485–7497, 1996). In this study, these two proteins were characterized in detail. In infected cells, both proteins localize not only to the viral membranes but also to tubular-cisternal membranes of the intermediate compartment, defined by the use of antibodies to either rab1A or p21, which colocalize with rab1A (J. Krijnse Locker, S. Schleich, D. Rodriguez, B. Goud, E. J. Snijder, and G. Griffiths, J. Biol. Chem. 271:14950–14958, 1996). Both proteins appear to reach this destination via cotranslational insertion into the rough endoplasmic reticulum, as shown by in vitro translation and translocation experiments. Whereas p16 probably spans the membrane twice, p8 is inserted into the membrane by means of its single NH_2-terminal hydrophobic domain, adopting a topology which leaves the C terminus exposed to the cytoplasm. Combined immunocytochemical and biochemical data show that p16 is a member of the inner of the two IMV membrane layers, whereas p8 localizes to both the inner and the outer membrane. These findings are discussed with respect to our model of IMV membrane assembly.

Vaccinia virus (VV), the best-characterized member of the *Poxviridae*, has a double-stranded DNA genome of about 200 kb that has been completely sequenced (10, 19). This genome encodes more than 200 proteins, of which approximately 100 are in the virion (9).

The morphogenesis of VV starts at about 3 h postinfection with the appearance in the cytoplasm of so-called virus factories, which are the sites of viral transcription and DNA replication (2). Within, or close to, these regions, and concomitant with the synthesis of the late (structural) proteins, crescent-shaped cisternal membranes emanate. Our data argue that these membrane structures are derived from the intermediate compartment (IC) between the endoplasmic reticulum (ER) and the Golgi complex (23, 34). From these crescents the spherical immature viruses (IVs) are made, which are the precursors of the first infectious form of the virus, the intracellular mature virus (IMV). A variable fraction of the IMVs then becomes enwrapped by a double bilayer derived from the trans-Golgi network to transiently form the intracellular enveloped virus (17, 30). This form of the virus is capable of polymerizing actin tails (4) which pushes the particle to the plasma membrane where it fuses, thereby releasing the three-membraned extracellular enveloped virus (EEV) into the extracellular space.

Our previous data have strongly suggested that the IMV, in contrast to most other enveloped viruses, acquires two membrane layers in one process (34). A similar mechanism has recently been shown to operate in the assembly of African swine fever virus, a member of the *Iridoviridae* that shares many similarities to poxviruses (3). By thin section electron microscopy (EM), however, the VV (IC-derived) membranes usually appear as one membrane profile, presumably because they are also tightly apposed that they appear as one membrane bilayer. The alternative explanation is that the VV-membrane is indeed a single bilayer, made de novo and independent of cellular template membranes (6, 7). From a cell-biological point of view, this latter model to explain VV membrane biogenesis would be highly unusual, having no precedent, and until now no molecular evidence has supported this model. Since our realization that the VV membranes may consist of two membrane layers, our major effort has been to provide additional (molecular) data for this model. At the molecular level we envision that the tight membrane apposition is generated by one, or several, virally encoded membrane protein(s) that interacts across the lumen of the IC to bring the two membranes into tight apposition, perhaps analogous to the process of tight junction formation. With this model in mind we have generated a comprehensive two-dimensional gel map of the major membrane and core proteins of the IMV (18). This map has enabled us to identify the gene products of A17L (p21), A14L (p16), and A13L (p8) as abundant membrane proteins of the IMV. Recently we have shown that the gene product of A17L (p21) fulfills all the criteria that could be predicted from our earlier models; it inserts into the rough ER (RER) in a cotranslational manner and localizes not only to the viral membranes but also to the IC in infected cells (23).

The gene products of A14L and A13L, two 16- and 8-kDa proteins, respectively, of the IMV, have been shown to behave like integral membrane proteins in infected cells; when post-

* Corresponding author. Mailing address: European Molecular Biology Laboratory, Meyerhofstrasse 1, 69117 Heidelberg, Germany. Phone: 49 6221 387508. Fax: 49 6221 387306. E-mail: KRIJNSE @EMBL-Heidelberg.de.

† Present address: Centre for Molecular and Cellular Biology, University of Queensland, St Lucia, QLD 4072, Australia.

nuclear supernatants of infected cells were subjected to treatment with Triton X-114, both proteins partitioned into the detergent phase, and both pelleted along with membranes following high-pH carbonate extraction (18). Moreover, when IMV preparations were treated with a mixture of Nonidet P-40 and dithiothreitol (DTT), both proteins were solubilized, a characteristic of VV membrane proteins (18). In a recent study (27) p16 (called p15 in that study) has been localized in infected cells using lowicryl-embedded thin sections. At relatively late times after infection, p16 labeled viral membranes as well as tubular-vesicular structures that accumulate close to the viral factories when the assembly of the crescent-shaped membranes is arrested (26, 27). These structures were probably part of the IC, since in single-labeling experiments they were also labeled by a marker protein of this latter compartment. In that study, however, it was not unequivocally shown that p16 accumulated in IC elements by double-labeling studies.

In the present study we have characterized the p16 and p8 proteins in more detail. In double-labeling experiments on thawed cryosections we show that at 6 h postinfection both proteins not only localize to the viral membranes, but they also accumulate in IC structures, as defined by an antibody to a well-characterized IC marker. Moreover, our data show that whereas p16 is an abundant membrane protein of the inner of the two IMV membrane layers p8 appears to be associated with the inner as well as the outer membrane.

MATERIALS AND METHODS

Viruses, cells, and antibodies. HeLa cells were grown as described previously (34). For most experiments (except when indicated), a mutant of WR, vRB12 was used, lacking the 37-kDa EEV protein and therefore deficient in making EEV (1). This virus was grown and purified as described previously in detail (18). The VV recombinant expressing the mouse hepatitis virus M (MHV-M) protein has been described before (21). A peptide matching amino acids 75 to 90 of the A14L gene was synthesized and coupled to keyhole limpet hemocyanin, and a peptide serum, called throughout this paper anti-p16-C, was generated, as described previously (5). For some experiments we also used a peptide serum described recently (27) that was raised against both amino acids 35 to 44 and 80 to 90 (27), referred to in this report as anti-p16-L/C. To characterize the gene product of A13L, a peptide antibody was raised against amino acids 49 to 67 (C terminus). The antibody to rab1 was a kind gift from Bruno Goud (29); the antibody to calnexin was a kind gift from Ari Helenius (16). The production of the antibody raised against the C terminus of p21 (gene A17L) has been described before (23). The use and generation of the NH_2- and C-terminal-specific antibodies to the MHV-M protein were described previously (21).

Cloning of the A14L and A13L gene. Two oligonucleotides, 5′ GGGGTAC CACCATGGACATGATGCTTATG 3′ and 3′ CTATAAAGGTACTTGATT AGTCCTAGGGGC 5′, were synthesized, corresponding to the 5′ and 3′ ends of the A14L gene, respectively. The oligonucleotides were chosen such that they introduced at the 3′ end a *Bam*HI and at the 5′ end a *Kpn*I restriction site. The A14L gene was amplified from genomic DNA extracted from WR-infected HeLa cells, using PCR. The PCR fragment of the expected size was extracted from the agarose gels. The fragment was cut with *Bam*HI and *Kpn*I and cloned into pBsSKII that was cut with the same enzymes. The A14L gene was sequenced and found to have one base substitution compared to the published Copenhagen strain sequence at position 217 (the sequence of the WR A14L gene has not been published yet). This base-pair substitution appeared to be a silent mutation. To clone A13L the following primers were used: 5′ CGGGGTACCACCATGAT TGGTATTCTTTTG 3′ and 5′ CGGGAATTCTGATTATACAGAAGATTTA AC 3′, corresponding to the 5′ and 3′ ends of the A13L and introducing a *Kpn*I and *Eco*RI site. The amplification and cloning into pBsSKII was as described for the A14L gene. Upon sequencing, the gene was found to be completely identical to the published Copenhagen strain sequence.

In vitro translations. In vitro translations in the presence or absence of micrococcal nuclease-treated microsomes (a kind gift from Katja Schroeder and Bernard Dobberstein) were carried out as described before (23). Translation of the MHV-M gene was carried out by using a previously described plasmid (21).

Protease treatment of cell lysates and purified IMV. For the protease treatment of infected cell lysates, HeLa cells were infected at a multiplicity of infection of 10 with the VV-MHV-M recombinant in the presence of rifampin. At 8 h postinfection the cells were scraped from the dish in phosphate-buffered saline and concentrated by pelleting for 10 min at 1,500 rpm in a Heraeus minifuge. The pellet was resuspended in potassium acetate (KOAc) buffer (25 mM HEPES [*N*-2-hydroxyethylpiperazine-*N*′-2-ethanesulfonic acid]-KOH, pH 7.4, 115 mM KOAc, 2.5 mM Mg acetate) diluted 1 in 10 in water. The cells were broken by eight strokes of a glass homogenizer, one-tenth of the total volume of 10× concentrated KOAc buffer was added, and the nuclei were pelleted in an Eppendorf centrifuge at 2,000 rpm. Protease K (Merck, Darmstad, Germany) and trypsin (Sigma) were added to the supernatant at a final concentration of 50 or 100 μg/ml, and the mixture was incubated for 30 min on ice or at 37°C, respectively. The digestion was terminated by the addition of phenylmethylsulfonyl fluoride (1 μl of a 40-mg/ml stock in isopropanol) to the protease K and aprotinin (1 μl of a 4-mg/ml stock) to the trypsin-treated samples. The samples were run on sodium dodecyl sulfate (SDS)–15% polyacrylamide gels and blotted onto nitrocellulose as described previously (8). The blots were probed with the anti-p16-C or p8 antibody both diluted at 1:10,000 or with NH_2-specific monoclonal antibody (1:300) or C-terminal-specific antibody (1:3,000) to the MHV-M protein. Protease K and trypsin digestions of purified IMV were carried out as described previously (5).

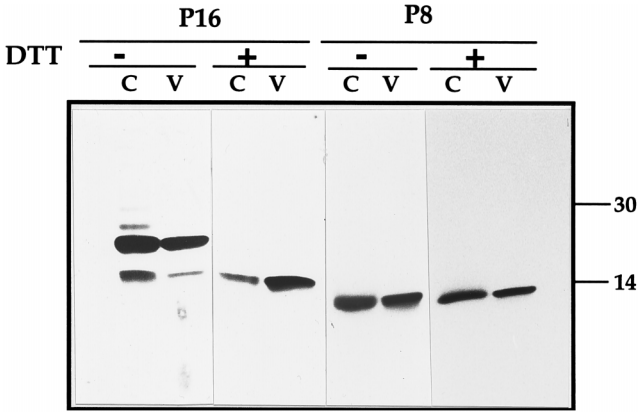

FIG. 1. Western blot analysis of anti-p16 and p8 antibodies. Purified IMV (lanes V) or cell lysates of rifampin-blocked infected cells (lanes C) were separated by SDS-PAGE with (+) or without (−) prior reduction with 100 mM DTT and 2% β-mercaptoethanol. The proteins were transferred onto nitrocellulose and probed with anti-p16-C or anti-p8. The positions of 14- and 30-kDa marker proteins are indicated on the right.

EM and preembedding labeling. HeLa cells infected for 6 h with the WR strain of VV were fixed and prepared for cryosectioning as described previously (8). Thawed sections were labeled with the p16-L/C antibody diluted 1:1,000 or were double-labeled with this antibody and antibodies to rab1 (1:40), to calnexin (1:10), or to p21 (1:150). The antibody to p8 was used at 1:200. Double labeling was carried out by the sequential protocol of Slot et al. (32), using a glutaraldehyde step between the two antibody and gold steps. The preembedding labeling after permeabilization was performed as described previously (23), using the antibodies at the same dilution as for the cryosections.

For negative staining EM, intact IMV or IMV treated for 30 min at 37°C with 20 mM DTT was adsorbed onto 300-mesh formvar- and carbon-coated grids. The virions were immunolabeled with the anti-p16-C or anti-p16L/C and anti-p8 antibodies as described previously (8).

Immunofluorescence in SLO-permeabilized cells. Immunofluorescence on streptolysin O (SLO)-permeabilized cells was essentially as described previously (23), using the C-terminal antibody to either p16 or p8 at a 1:1,000 dilution. The secondary goat anti-rabbit antibody coupled to fluorescein isothiocyanate was from Dianova (Dainova-Immunotech GmbH, Hamburg, Germany). Viral DNA was labeled with Hoechst dye (Sigma; no. 33258) at 5 μg/ml.

RESULTS

The A14L gene encodes a protein of 90 amino acids with a predicted molecular size of 10 kDa, while the amino acid sequence of the A13L gene predicts an 8-kDa protein. After SDS-polyacrylamide gel electrophoresis (PAGE), however, both proteins migrate at considerably higher molecular weights, as observed previously (27, 36). As a consequence of its migration after SDS-PAGE, the gene product of A14L has been called p16, while A13L was previously referred to as p8 (18). We have adopted this terminology throughout this report. Previous studies have estimated the molecular size of the A14L gene product to be 15 kDa (27). This small difference in molecular size might be due to the use of different SDS-PAGE conditions.

Two antibodies recognizing p16 were used. The first was a

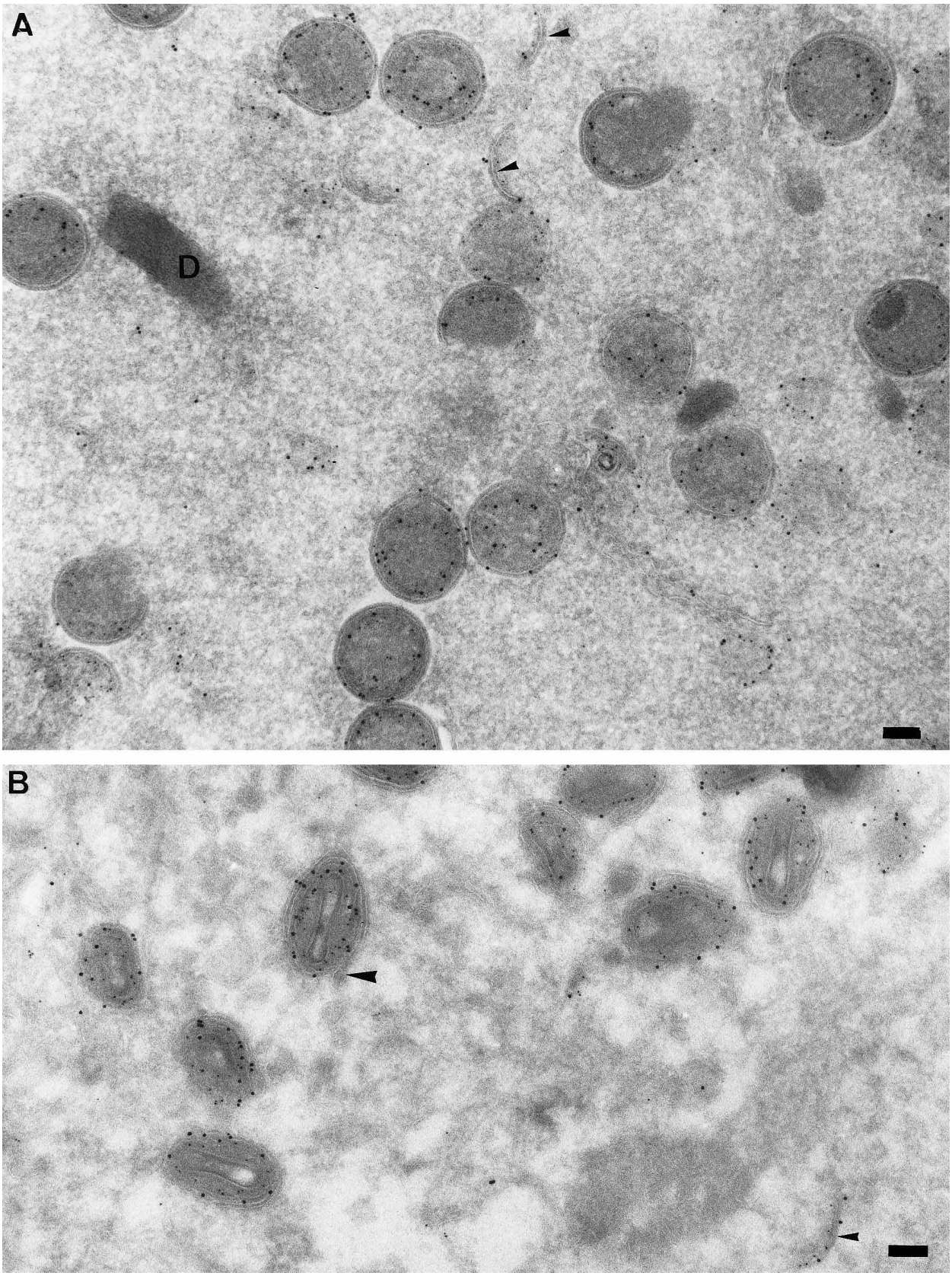

FIG. 2. Thawed cryosections of HeLa cells infected for 6 h with VV WR. The sections were double labeled with anti-p16 (5-nm gold) and anti-p21 (10-nm gold). The small arrowheads in both panels show crescents, while the large arrowhead in panel B shows the (unlabeled) wrapping cisterna during the process of the formation of the intracellular enveloped virus, the intracellular form of the EEV. D, viral DNA. Bars, 100 nm.

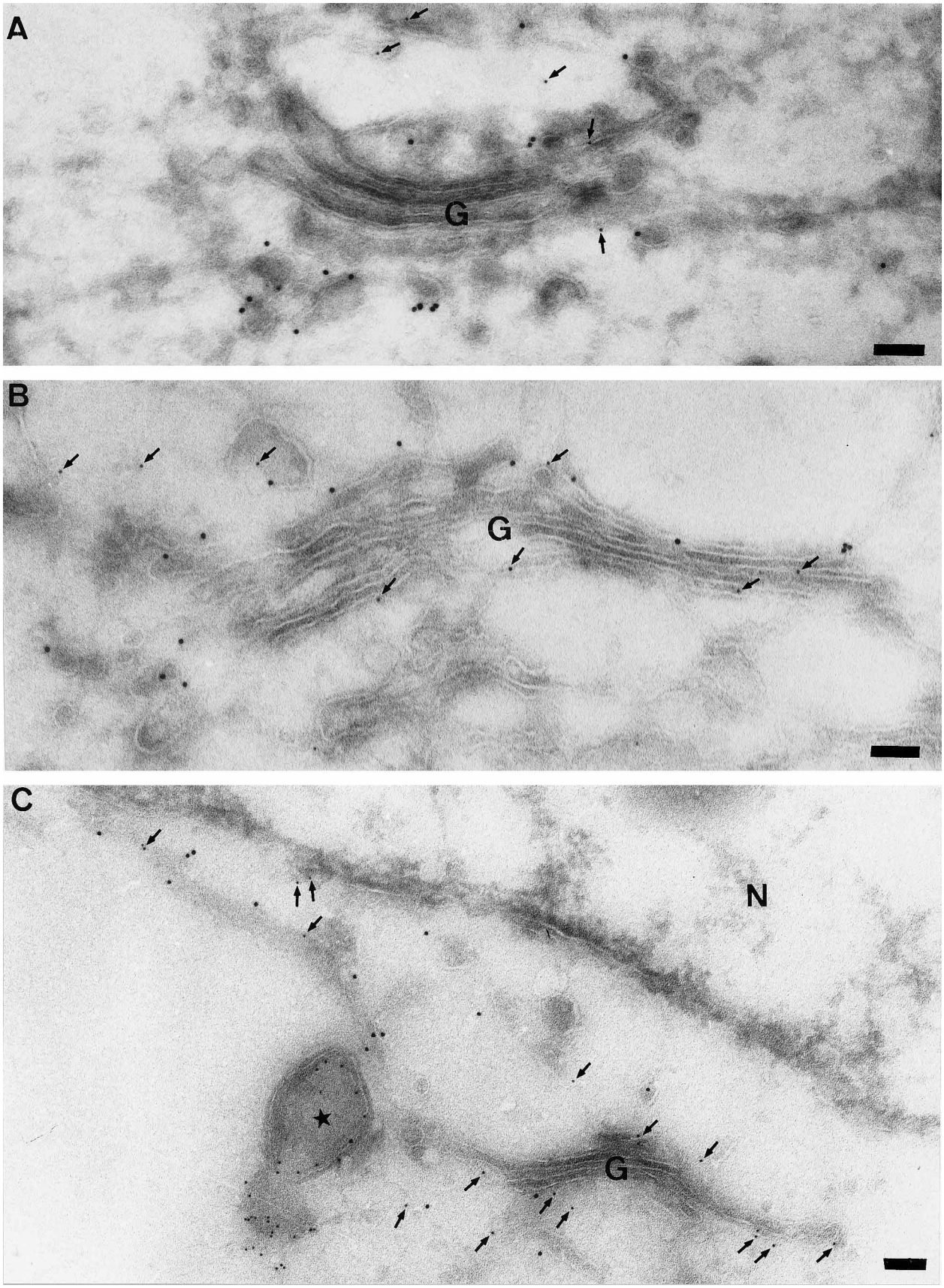

FIG. 3. Double-labeling for anti-p16 (5-nm gold, arrows) and anti-rab1 (10-nm gold, unlabelled). (A, B, and C) The pattern of overlap of the two proteins in the (mostly) periphery of the Golgi stack (G). The central cisternae are essentially unlabeled for both antigens. In panel C, which is from an SLO-permeabilized cell, two gold particles for p16 are indicated on the nuclear envelope and colocalization of p16 and rab1 are also seen in cisternal elements of the intermediate compartment adjacent to the Golgi. N, nucleus. The star shows an IV that is strongly labelled for p16. Bars, 100 nm.

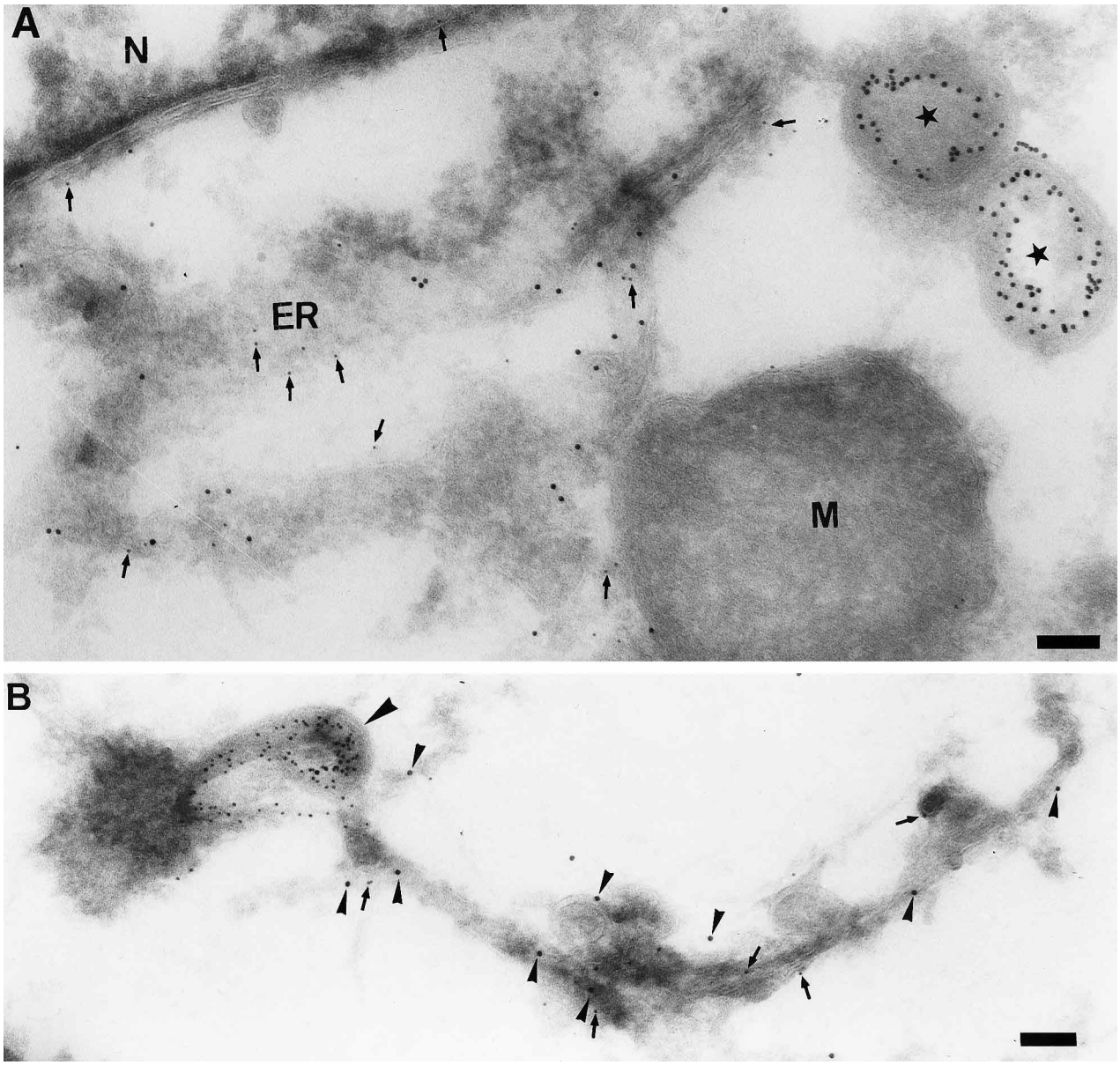

FIG. 4. Double labeling for calnexin and p16. (A) Calnexin (5-nm gold, arrows) and p16 (10-nm gold). Both antigens are seen in the nuclear envelope and, more prominently, in the ER. The stars indicate IVs labeled for p16. N, nucleus; M, mitochondrion. (B) SLO-permeabilized cell. Calnexin, small arrowheads, 10-nm gold; p16, arrows, 5-nm gold. Apparent continuity is seen between a double-labeled cisternal element that is continuous and a crescent (large arrowhead) which is heavily labeled for p16. Bars, 100 nm.

recently described peptide antibody that was raised against two different peptides (amino acids 35 to 44, corresponding to a hydrophilic stretch that separates two hydrophobic domains, and amino acids 80 to 90, corresponding to the extreme C terminus) (27). The second was raised against a peptide sequence covering amino acids 75 to 90 (extreme C terminus). These two antibodies are referred to here as p16-L/C and p16-C, respectively. For the characterization of p8 we raised an antibody to amino acids 49 to 67 of the A13L sequence (C terminus).

Figure 1 shows a Western blot of cell lysates of rifampin-blocked infected cells as well as of purified virus probed with the anti-p16-C and the anti-p8 antibodies. Since rifampin is known to reversibly block viral assembly but not viral late protein synthesis (15, 24), this drug can be used to assess whether VV proteins migrate differently upon SDS-PAGE (e.g., due to processing) in the absence of virus formation. Samples were run under reducing and nonreducing conditions. As before (27), the p16 antibody recognized a 16-kDa as well as a 25-kDa band. This latter form most likely represents a disulfide-bonded dimer of the 16-kDa form, as judged by the absence of the 25-kDa band when samples were reduced prior to analysis (see also reference 27). The migration of p8 was the same whether analyzed with or without reduction, and the antibody in all cases recognized a single band with an approximate molecular size of 12 kDa.

By indirect immunofluorescence of cells that were infected for 6 h, both antibodies recognized distinct punctate structures

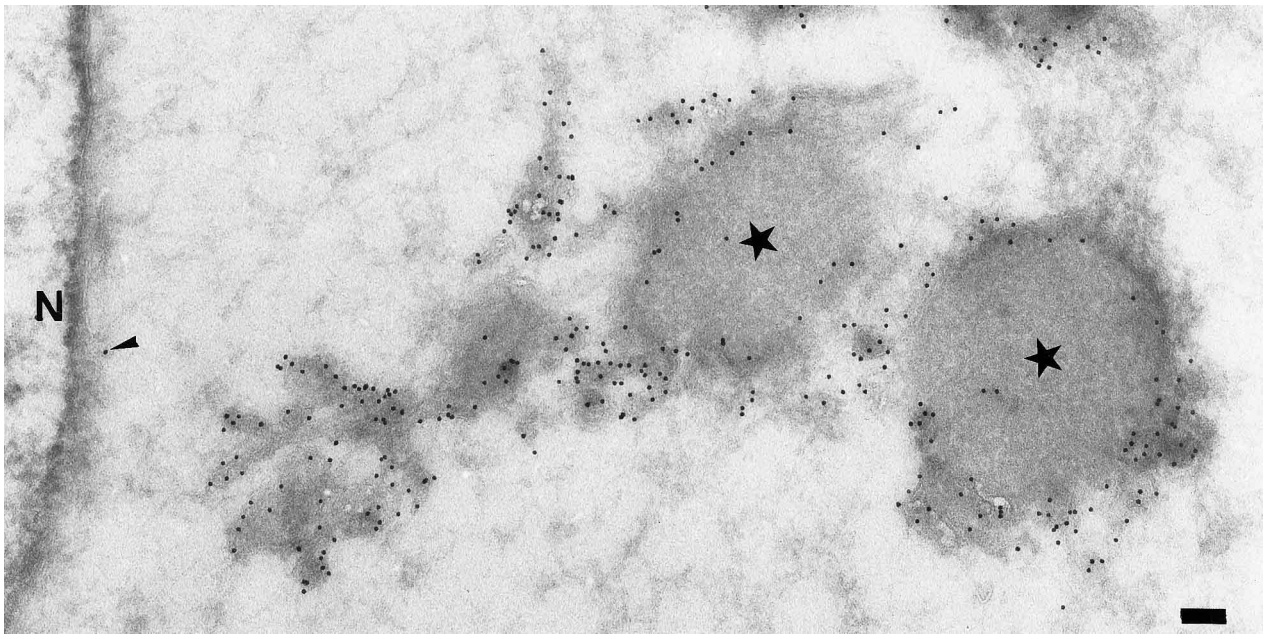

FIG. 5. Single labeling for p16 of a HeLa cell infected with VV in the presence of rifampin. Note the strong labeling in the membrane structures surrounding the rifampin bodies (stars). A single gold particle is on the nuclear envelope (arrowhead). N, nucleus. Bar, 100 nm.

in the perinuclear region of the cell, to a great extent overlapping with the regions of DNA labeling (see Fig. 12A, B, D, and E), typical of the viral factories (23). In contrast to the more uniform DNA labeling, the labeling for both antibodies was distinctly punctate.

Localization of p16 and p8 in infected cells. To study p16 and its role in VV assembly we first localized the protein by immunogold EM by using thawed cryosections of aldehyde-fixed cells. In all cases, cells were infected for 6 h prior to fixation and p16-L/C was used for labeling the peptide serum. The localization of p16 is first described in double-labeling studies with p21 (A17L), a membrane protein we have recently shown to be restricted to the inner membrane of the IV and IMV, as well as to the ER and the IC (23). As shown in Fig. 2, p16 and p21 were indistinguishable both in the IV (Fig. 2A) and the IMV (Fig. 2B), labeling mostly the inner aspect of both the IV and IMV membranes. Occasionally the central parts of the IVs seemed to be labeled. However, the pattern of labeling was always clearly different from labeling with antibodies to core proteins, which uniformly label the central part of the IVs (8). We therefore assume that the more central labeling with the antibodies to both p16 and p21 relates to the plane of sectioning through the spherical IVs, as well as the fact that in the cryosection method we use, the labeling is usually restricted to the section surface (11).

When analyzing cellular membranes, p16 localized mainly to IC structures, as shown by its at least partial colocalization with rab1, which has previously been localized to the IC (14, 29) (Fig. 3). Consistent with our earlier studies on IC-localized proteins (20), the p16 labeling often extended to the Golgi complex, labeling mostly one side of the stack (or sometimes both, depending on the plane of section through the stack), while the central cisternae of the stack was essentially unlabeled (Fig. 3A and B). Although the labeling of the structures defined as IC was the most prominent, small but significant amounts of p16 labeling were also associated with the nuclear envelope (see Fig. 5 and 6) and with the ER, where it colocalized with calnexin, a marker protein that localizes mainly to the RER (22) (Fig. 4).

In cells that had been treated with rifampin, a drug that blocks VV assembly prior to formation of the IV (24), p16 strongly labeled the membranes surrounding the viral factories (that accumulate under these conditions) as well as membrane tubules emanating from them (Fig. 5). These tubular-cisternal structures, best seen after a preembedding approach (see below), were described before (34).

We subsequently established the localization of p8 by comparing it to p16 in double-labeling studies. The overall labeling of p8 appeared much lower than that for p16, most likely due to the lower affinity on cryosections of the p8 antibody. This was irrespective of whether the p8 antibody was used first or second in the sequential double-labeling method we employed, nor did the size of gold (5 and 10 nm) specific for p8 make any difference (not shown). From systematic sampling of these preparations, it became clear that p8 and p16 colocalized to the same intracellular tubular-cisternal structures of the IC that extended to elements on one side of the Golgi stack (Fig. 6 and 7A), whereas the nuclear envelope as well as the RER had a low level of specific labeling for both proteins. In addition to labeling IC elements, p8, like p16, localized to the membranes of the IVs (Fig. 7B to D and 8) and IMVs (Fig. 6C and 8). On cryosections, the great majority of the labeling for both proteins was found associated with the inner membrane of both the IV and the IMV (Fig. 8). As will be shown below, for p8 these latter results are inconsistent with the data from the preembedding labeling EM. Taken together, these immunocytochemical data show that p16 and p8 localize as expected for two IMV membrane proteins; they not only label the viral but also the intracellular membranes of the IC that, from our previous studies, are functionally proximal to the Golgi complex.

p16 and p8 insert into microsomes in a cotranslational manner. Previous experiments have shown that p16 and p8 behave like integral membrane proteins in several respects.

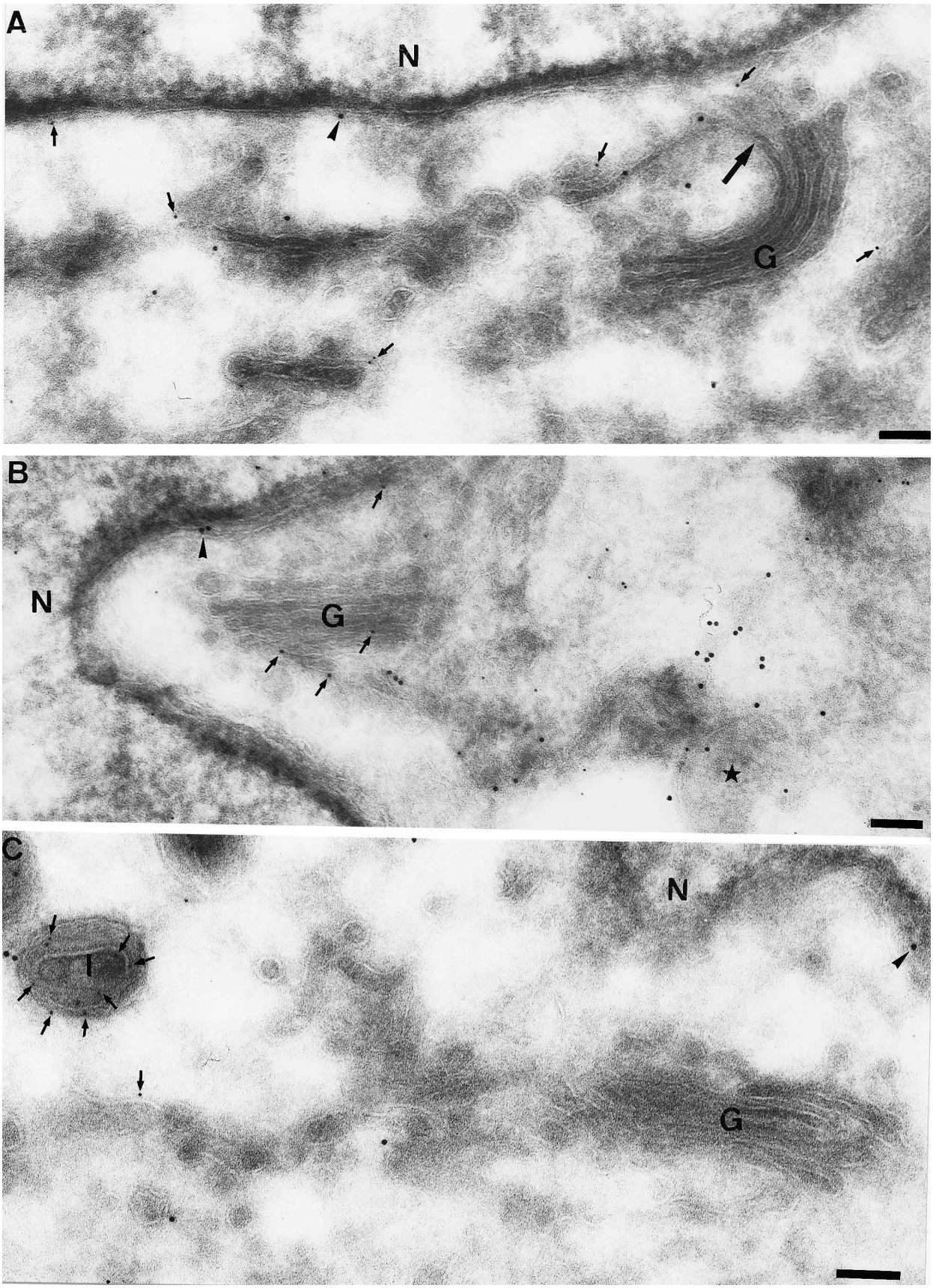

FIG. 6. Thawed cryosections of HeLa cells double labeled for p8 and p16. All three micrographs emphasize the fact that whereas the bulk of the Golgi stack (G) is devoid of labeling for both proteins the labeling is found in characteristic IC elements that are, in part, in close apposition to the *cis* side of the Golgi stack. In panel A the large arrow indicates a *cis* cisterna that peels off the stack to give p10- and p16-positive elements. In panels A and C p8 is labeled with 10-nm gold (arrowheads) and p16 is labeled with 5-nm gold (small arrows); in panel B p16 is labeled with 10-nm gold (arrowheads) and p8 is labeled with 5-nm gold (small arrows). Note the small amount of labeling for both proteins in the nuclear envelope. N, nucleus. The star in panel B indicates an IV, while the I in panel C shows an IMV. Bars, 100 nm.

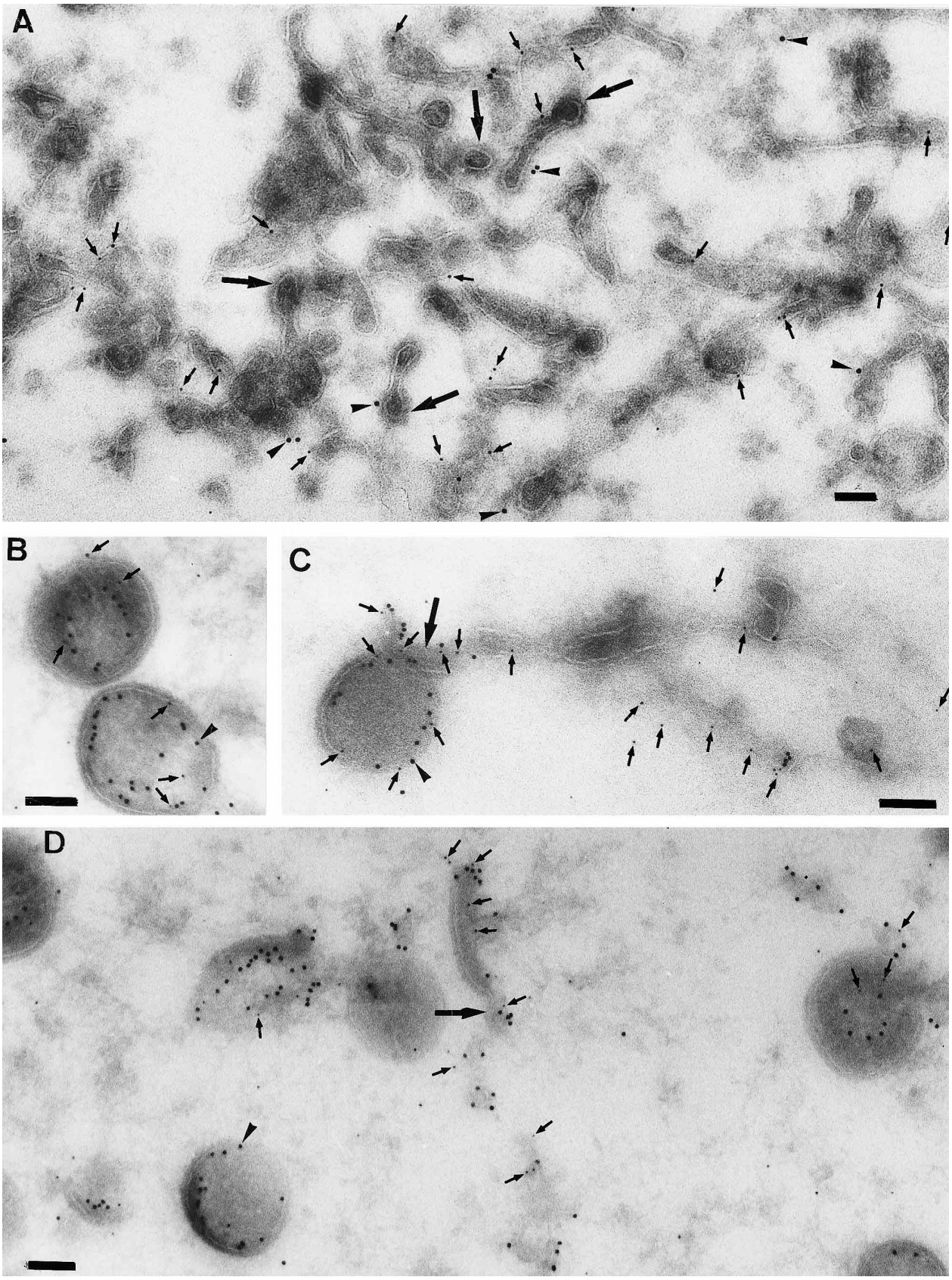

FIG. 7. Thawed, cryosections of HeLa cells double labeled for p8 and p16. (A) An extensive array of IC elements labeled for both proteins: p16 (5-nm gold, small arrows) and p8 (10-nm gold, arrowheads). The large arrows indicate putative COP-I buds that are known to be enriched on the IC. Panels B, C, and D show labeling for both p16 (10-nm gold, arrows) and p8 (5-nm gold, small arrows) on crescents and IVs. Note that the great majority of the labeling for both proteins appears to be on the inner aspect of these structures. The large arrows in panels C and D show contiguities (panel C) or continuity between the crescent and what are probably tubular elements of the IC. Bars, 100 nm.

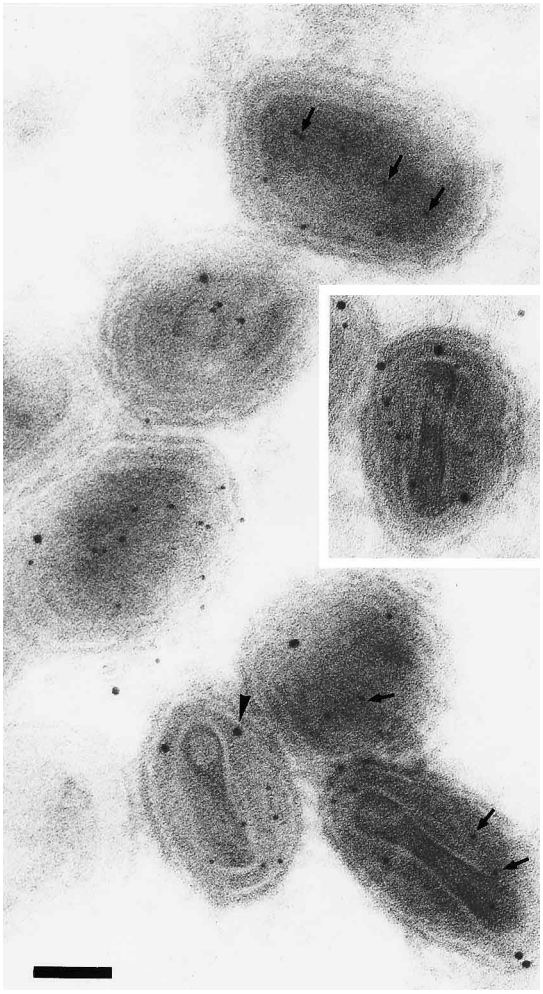

FIG. 8. Double labeling for p8 (10-nm gold, arrowhead) and p16 (5-nm gold, small arrows). Labeling of sections through IMV particles. Note the absence of labeling for both proteins on the outer membrane. Bar, 100 nm.

They can, for instance, be extracted from the IMV by using a mixture of Nonidet P-40 and DTT (18), a characteristic of membrane proteins of the IMV. Hydrophobicity plots of p16 showed that it contains two stretches of hydrophobic amino acids long enough to span a membrane, which are predicted to be α-helical (23 and 24 amino acids long, respectively) (27). In fact, the entire NH_2 terminus of p16 is hydrophobic, since the first putative (α-helical) transmembrane domain is preceded by another hydrophobic stretch of 10 amino acids. The two predicted membrane-spanning domains are interrupted by 10 residues of a more hydrophilic nature. The C-terminal part (22 amino acids long) following the second putative membrane spanning segment is again hydrophilic. The simplest scenario is that this protein crosses the membrane twice, having the NH_2 and C termini on the same side, with the stretch between the two hydrophobic segments being on the opposite side of the membrane.

p8 has a single hydrophobic domain at its NH_2 terminus (21 amino acids long) that might serve as a membrane anchor. Since newly synthesized p21 (A17L) is inserted into the RER and appears to be retained at the functional IC-Golgi border, it was logical to ask whether p16 and p8 behaved similarly. We therefore investigated whether the two proteins also inserted into RER membranes and whether their insertion was co- or posttranslational. p16 and p8 were translated in vitro by using a reticulocyte lysate system in the presence or absence of rough microsomes. As shown in Fig. 9 it seems clear that both proteins do indeed associate with microsomal membranes, but only when the microsomes were present at the onset of translation, which is cotranslational.

During these experiments we noticed that the membrane-integrated p16 migrated slower than the untranslocated protein. While this latter form comigrated with the monomer of p16 made in infected cells (not shown; 23a), we are currently studying the modification that leads to the shift in molecular weight upon membrane insertion of p16 in more detail (see Discussion).

Topology of p16 and p8 in vitro. Experiments were next carried out to determine the membrane topology of both proteins in vitro. Based on its predicted membrane association described above, p16 could adopt two possible topologies. The first is that the loop separating the transmembrane domains is cytosolic, with both the NH_2 and C termini being lumenally disposed. The second possibility is that the NH_2 and C termini are cytosolic and the loop is lumenal. Protease digestions on p16 translated in vitro in the presence of microsomal membranes would, in the first model, be expected to digest the loop, yielding two pieces of approximately 34 and 46 residues long. The alternative topology would predict the loss of both the NH_2 and C termini, leaving a single loop fragment of 58 amino acids. However, when p16 synthesized in vitro in the presence of microsomes was digested with either protease K or trypsin we observed a complex pattern of breakdown products upon SDS-PAGE that were not easy to interpret (data not shown).

The p8 sequence contains one hydrophobic domain at its extreme NH_2 terminus and could either adopt a topology exposing its C terminus toward the cytoplasm or toward the lumen. When p8 was translated in vitro in the presence of microsomes it could be immunoprecipitated with an antibody to its C terminus. In contrast, after protease digestions this

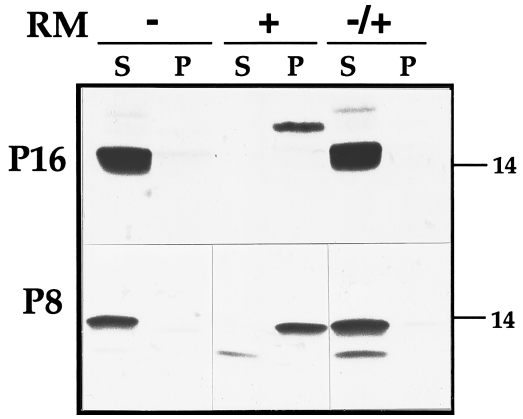

FIG. 9. p16 and p8 insert into rough microsomes in a cotranslational manner. p16 and p8 were translated in vitro in the presence (+) or absence (−) of rough microsomes (RM). The membranes were pelleted through sucrose, the soluble proteins (lanes S) were immunoprecipitated from the supernatant by using the C-terminal antibodies to either p16 or p8, and the membrane-integrated proteins (lanes P) were recovered from the pellet. To test for posttranslational insertion, the in vitro translation reaction was carried out without microsomes and at the end of translation, cycloheximide and microsomes were added and the reaction was allowed to proceed for an additional 45 min (RM −/+). The p8-reactive, faster migrating band, most prominent in the supernatant of samples in which the microsomes were added after translation, is probably the product of internal initiation or premature termination of translation. The position of the 14-kDa marker protein is on the right.

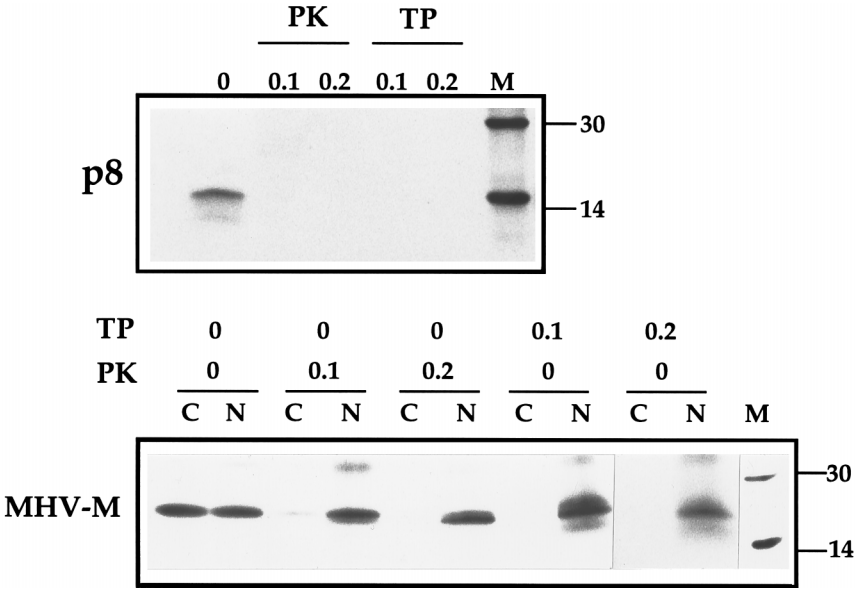

FIG. 10. Topology of p8 in vitro. p8 and the MHV-M proteins were translated in vitro in the presence of rough microsomes and either not treated (lane 0) or treated with 0.1 (lane 0.1) or 0.2 (lane 0.2) mg of protease K (PK) or trypsin (TP) per ml. Digestions for 30 min on ice or 30 min at 37°C, respectively, were followed by immunoprecipitation with the anti-p8 antibody or antibodies to the NH_2 (lanes N) or C terminus (lanes C) of the MHV-M protein. Lane M, marker proteins for which the 14- and 30-kDa positions are indicated.

reactivity was lost, arguing that the C terminus is cytosolically exposed (Fig. 10). As a control for these protease treatments, we used the MHV-M protein. The topology of this latter protein has been well established, having its NH_2 terminus lumenal and its C terminus cytosolic. As before (21), we found that after protease treatment its NH_2 terminus was protected while its C terminus was lost (Fig. 10).

Topology of p16 and p8 in infected cells. Since the in vitro data on p16 gave results that were difficult to interpret, we decided to investigate the topology of p16, as well as that of p8, in infected cells in two independent ways. First, postnuclear supernatants of infected and rifampin-blocked cells were subjected to protease treatment, followed by Western blot analyses, using the C-terminal-specific antibodies to either p16 or p8. Rifampin was used to prevent IV/IMV assembly, in order to avoid the situation in which cytosolically exposed epitopes of the proteins might end up inside the virion during its assembly and therefore be inaccessible to proteases. Under our experimental conditions, p16 appeared partially protected against proteases (Fig. 11). Probing the same blot with anti-p8 antibodies revealed that reactivity to the antiserum was completely lost after digestion (Fig. 11), again suggesting, in agreement with the in vitro experiments, that the C terminus is cytosolically disposed. As a control we again used the MHV-M protein, expressed by using a VV recombinant (21) which showed, as predicted, that its NH_2 terminus was protected while the C terminus was digested (Fig. 11).

An independent approach to investigate the topology of p16 and p8 consisted of subjecting VV-infected cells to indirect immunofluorescence analysis after SLO permeabilization with the C-terminal antibodies (21). In this assay, the plasma membranes of infected and rifampin-blocked cells were selectively permeabilized with SLO at 6 h postinfection. This permeabilization step will allow antibodies to diffuse into the (unfixed) cells and recognize cytosolically exposed epitopes (21). As a control we again used the MHV-M protein which has its C terminus cytoplasmic and its NH_2 terminus lumenal. Using specific antibodies to the MHV-M protein expressed using a

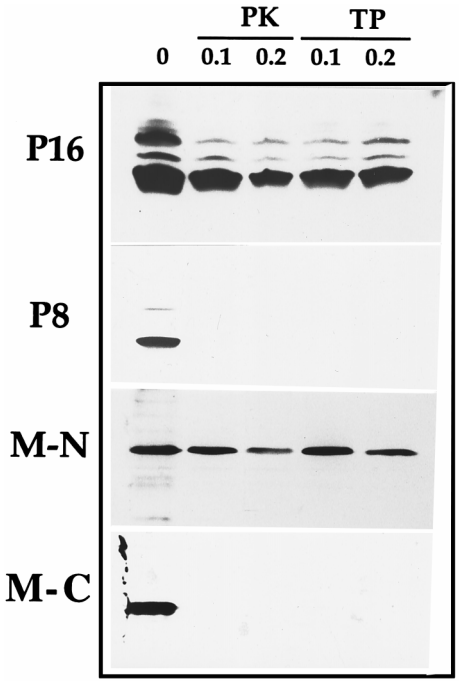

FIG. 11. Protease digestions on cell lysates of infection rifampin-blocked HeLa cells. Postnuclear supernatants of rifampin-blocked cells infected with a VV recombinant expressing the MHV-M protein were prepared at 8 h postinfection. The cell lysates were not treated (lane 0) or treated with a final concentration of 0.1 mg/ml (lane 0.1) or 0.2 mg/ml (0.2) of protease K (PK) on ice or trypsin (TP) at 37°C. The samples were subjected to SDS-PAGE, and the proteins were transferred to nitrocellulose. Digestion of p16 and p8 was detected by probing the blots with the respective C-terminal antibodies, while the digested parts of the MHV-M protein were assessed by using the NH_2-terminal (M-N)- and C-terminal (M-C)-specific antibodies. Since the samples were reduced with β-mercaptoethanol only, the p16 appears in monomer, dimer, and intermediate forms that will be described elsewhere (23a).

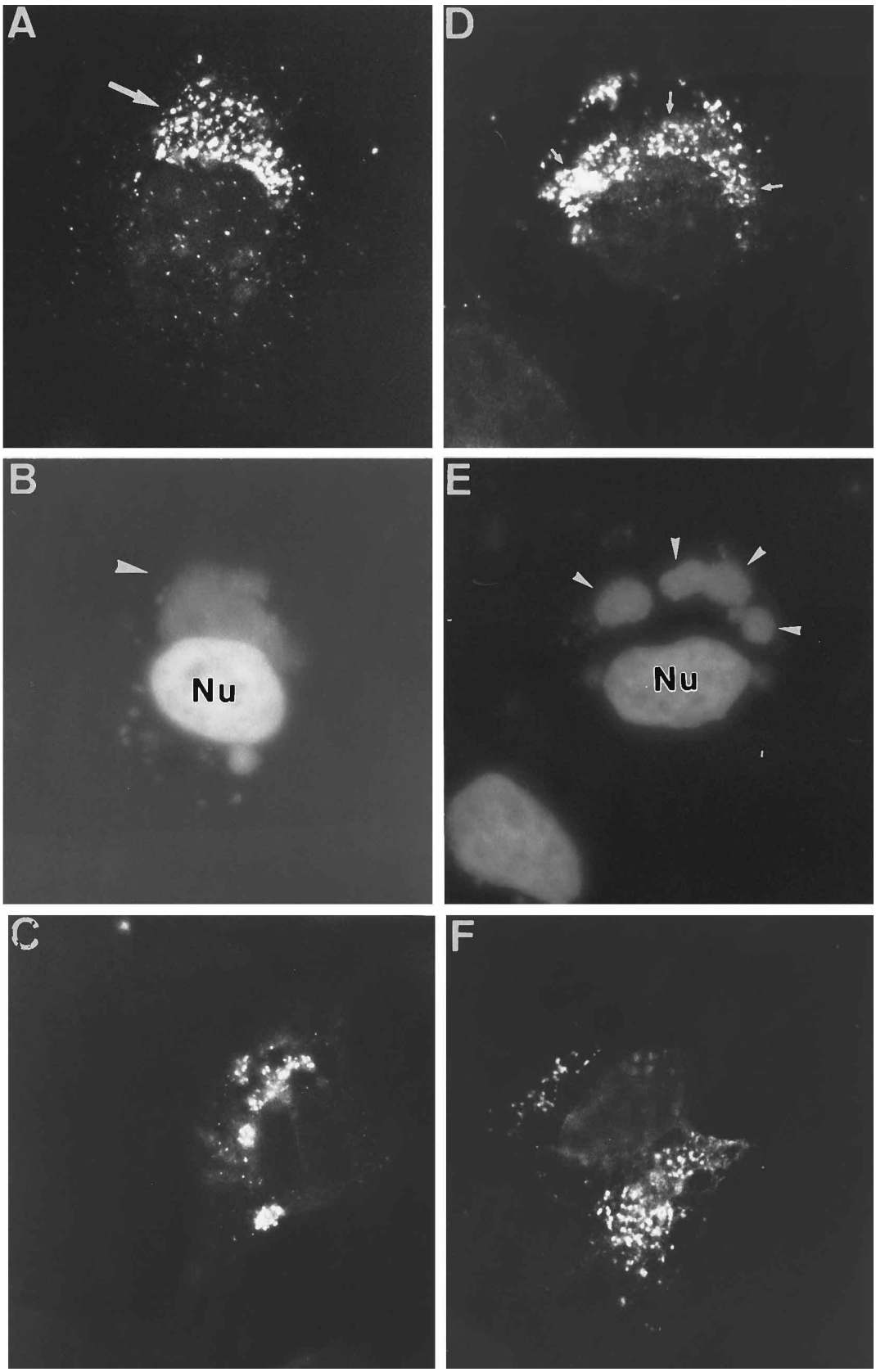

FIG. 12. Indirect immunofluorescence on SLO-permeabilized infected cells. (A, B, D, and E) Indirect immunofluorescence of infected HeLa cells fixed with methanol at 6 h postinfection. Typical punctate labeling is seen in panel A for p16 (large arrow) and in panel D for anti-p8 labeling (small arrows) that, in both cases, overlaps with the region of DNA labeling in panels B and E (arrowheads). Nu, nucleus. (C and F) Rifampin-blocked cells, permeabilized with SLO at 6 h postinfection and incubated with the anti-p16-C (panel C) and anti-p8 (panel F) antibodies before fixation and further incubation with a goat anti-rabbit antibody coupled to fluorescein isothiocyanate. Note that for both antibodies a distinct perinuclear punctate labeling can be seen that is indistinguishable from that seen in methanol-fixed cells and that is typical of the viral factories (arrows in panels A and D).

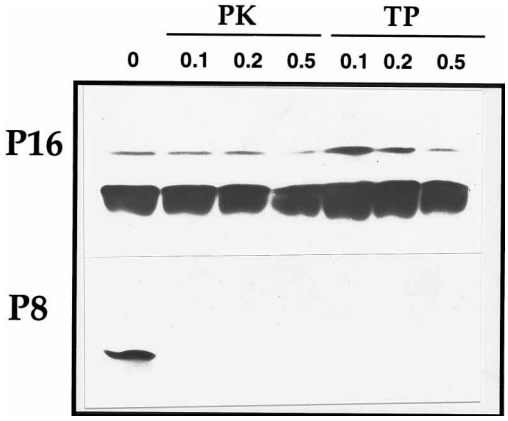

FIG. 13. Protease digestions of purified IMV. Purified IMV preparations were subjected to protease K (PK) or trypsin (TP) treatment at 0.1, 0.2, and 0.5 mg/ml final concentrations. Digestion was assayed by Western blotting, using anti-p16-C and anti-p8.

VV recombinant, the C-terminal antibody showed a strong labeling of a Golgi-like perinuclear structure, while the NH_2-terminal antibody did not show any labeling under these conditions (21) (not shown). Using antibodies that recognize only the C-terminal domains of p16 and p8, we could detect strong fluorescence labeling in both cases. Both antibodies labeled distinct punctate structures indistinguishable from the labeling seen in infected cells that were fixed without prior SLO permeabilization (compare Fig. 12A and D to 12C and F) and that overlapped with regions enriched in DNA (not shown).

Thus, in infected cells, p16 apparently exposes its C terminus toward the cytoplasm (see Discussion). p8, as assessed by the protease digestions as well as by the SLO experiment, adopts a topology both in vitro as well as in infected cells in which the C terminus is cytosolically oriented.

Localization of p16 and p8 in IMV. Next, we determined whether p16 and p8 were present in the inner or outer membrane of the IMV. We used three independent approaches to this question. First, purified IMV was digested with either protease K or trypsin and the extent of proteolysis analyzed by Western blotting. As shown in Fig. 13, p16 was essentially unaffected by either protease, consistent with a location of the C terminus within the particle. In contrast, reactivity to the C-terminal antibody to p8 was completely lost after proteolysis (Fig. 13), suggesting that p8 is present in a location where it is easily accessed by proteases, e.g., the surface of the IMV (but see Discussion).

Immunolabeling of intact IMVs followed by negative-staining EM gave results that were consistent with the protease results. No significant labeling of intact virions was detected with the two anti-p16 antibodies (Fig. 14C and D), while labeling with anti-p8 revealed 10 to 20 gold specks per particle (Fig. 14A; Table 1; for a rough comparison these numbers can be compared with the number of immunogold particles obtained per IMV with the outer membrane-exposed p14 (40 gold particles per IMV) or p32 (18 gold particles per IMV) (35). Strikingly, the average labeling for p8 increased about twofold after treating the IMVs with 20 mM DTT (Fig. 14B; Table 1; see Discussion).

Although there was no access of anti-p16 antibodies to their antigen in either untreated or DTT-treated IMVs, a small number (less than 1%) of DTT-treated IMVs showed labeling of tubular membrane elements that spilled out of the particle (Fig. 14E). We interpret these data to mean that upon DTT treatment the cisternal membranes in these particles begin to detach from the core (28), but only occasionally do they detach such that the inner membrane (and consequently the C terminus of p16) becomes exposed to its antibody.

Finally, we addressed the question of topology in the virus by preembedding immunogold labeling, an approach we have used previously for localizing both p21 (A17L) and p65 (D13L) to the inner of the two IMV membranes (23, 33). Infected cells were permeabilized at 6 h postinfection, briefly fixed with 4% paraformaldehyde, and subsequently incubated with anti-p16-L/C or anti-p8, followed by protein A-gold and embedding into Epon. As is evident from Fig. 15, the labeling for p16 was mostly associated with the inner of the two IV membranes (Fig. 15A), completely in agreement with the results described above as well as with the labeling on cryosections. Upon quantitative analysis, 95% of the gold particles were located on the inner side of the IVs (Table 2).

In these preembedding labeling experiments discrete tubular structures that labeled heavily for p16 became apparent. Since these structures were often connected to the membranes of the IVs, the crescents (Fig. 15), as well as to the ER (Fig. 15B), they most likely represent elements of the IC, described previously (34), which have high concentrations of p16. They are probably equivalent to the tubular structures that emanate from the rifampin bodies (see above at Fig. 5). For p8 the situation was different; while the use of cryosections had shown that essentially all of the antigen was on the inner aspect of the IVs, after preembedding labeling both sides of these structures were labeled (Fig. 16A and B and Table 2). Quantitative data showed in fact that the outer membrane was preferentially labeled, with 70% of the total gold being associated with this side of the IV membrane. This result was essentially consistent with the above-mentioned protease data, showing that the majority of p8 is accessible to proteases applied to the outside of the IMV. Moreover, by preembedding labeling the outer surface of the IMVs was significantly labeled (Fig. 16C). The extent of this labeling on thin sections was roughly equivalent to the numbers seen on intact virus by negative staining EM (Table 1).

DISCUSSION

In order to provide a framework for studying VV assembly at the molecular level, we have recently established a two-dimensional gel map of the major membrane and core proteins of the IMV (18). This map has enabled us to identify the A17L (p21), A14L (p16), and A13L (p8) gene products as the three most abundant membrane proteins of the IMV. Recent studies of the gene product of A17L, an abundant 21-kDa membrane protein, have shown it to be essential for morphogenesis (26, 37). This protein has a substantial part of its sequence buried in the membrane, since it may span the membrane four times, and is found mostly in the inner of the two IV membrane profiles (23). Moreover, this protein was the first of the IMV membrane proteins that was found to be inserted into the RER membrane in a cotranslational manner, following the general rules of cellular (and viral) membrane proteins.

In this study we have characterized the other two abundant membrane proteins, p8 and p16. We show that these proteins also insert into the RER in a cotranslational manner and are targeted to and retained in IC membranes in infected cells, since they did not label the bulk of the Golgi complex membranes. In fact, the complete set of our observations on the ER-Golgi boundary in this study agreed fully with our previous analyses (12–14, 20), arguing strongly that the most distal domain of the IC has a cisternal organization which seems to be

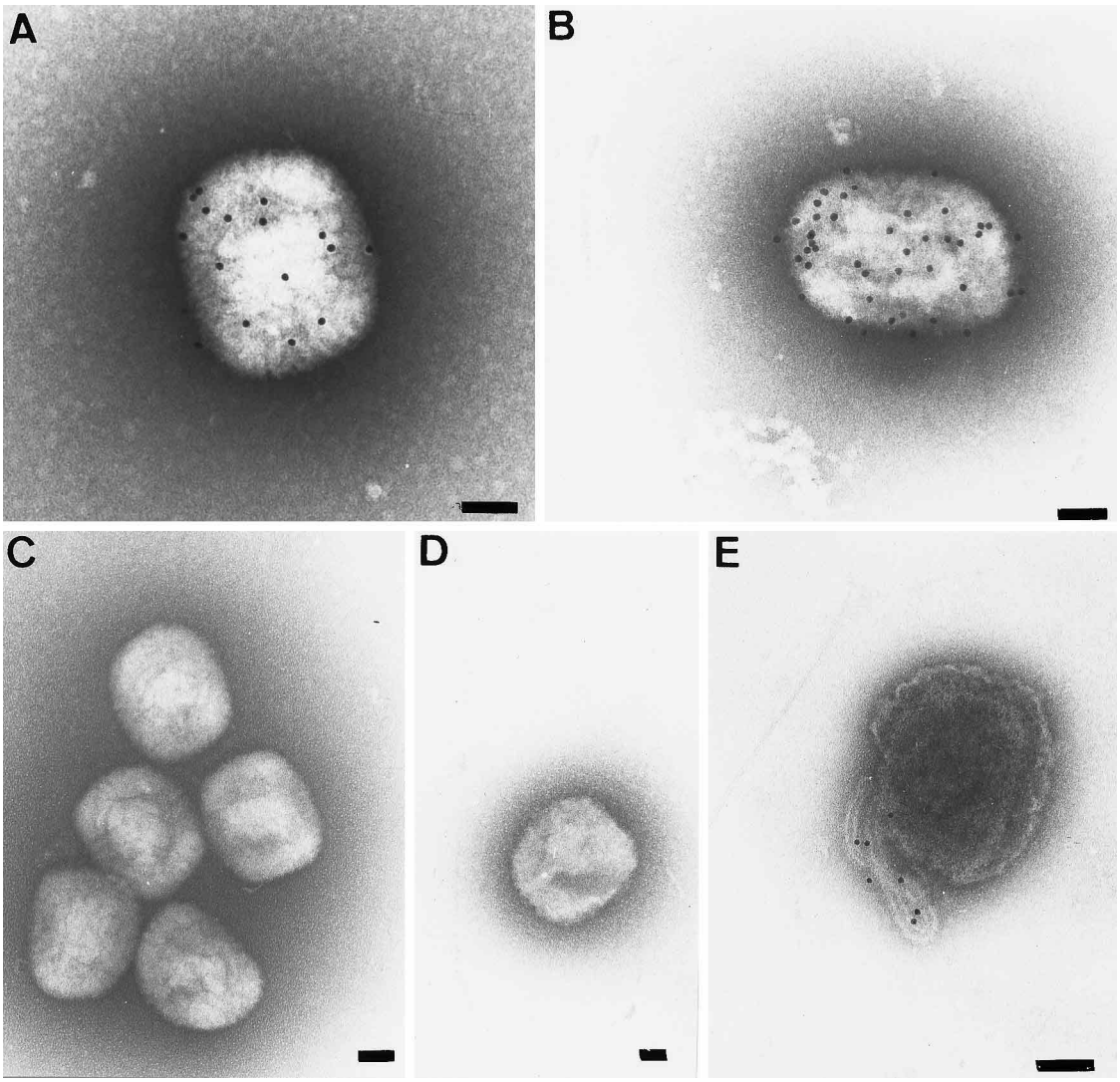

FIG. 14. Negative staining EM of intact and DTT-treated IMV. (A and C) Untreated IMVs labeled with anti-p8 (panel A) or anti-p16-C, followed by staining with 2% ammonium molybdate. (B, D, and E) DTT-treated IMVs labeled with anti-p8 (panel B) and anti-p16-C (panel D and E). Note that in panel D the DTT-treated IMV is essentially unlabeled by the p16 antibody; in panel E, however, the membrane cisterna that is peeling off the core exposes what is most likely the inner membrane that labels for p16. Bars, 100 nm.

physically glued to the *cis* side of the Golgi stack (see, for example, Fig. 3 and 6A).

A striking observation we have made here, and previously (for example, see reference 27), was that both p8 and p16 migrate in SDS-polyacrylamide gels at considerably higher molecular weights than those predicted from their amino acid sequence. p16, a protein with a molecular size of 10 kDa migrated as a 16-kDa protein, while p8 with a molecular size of 8 kDa always ran at approximately 12 kDa. Two obvious reasons could explain the aberrant migration; these may be a consequence of their secondary structures, although those structures would have to resist denaturation by SDS and DTT. An alternative explanation is that p16 and p8 acquire modifications that increase their molecular weights. p16, for instance, has been shown to be phosphorylated as well as myristylated (27). Modifications added to p8 have not been described and were not investigated in this study, but we have noted previously that on two-dimensional gels p8 migrates at pI values that are 2 units less than predicted (predicted pI is 10, calculated pI is 8; see reference 18). Phosphorylation could account for such a (acidic) shift in pI.

Having a hydrophobic stretch of 21 amino acids at its NH_2 terminus, p8 adopts a topology whereby its C terminus is cy-

TABLE 1. Labeling with anti-p8 of intact and DTT-treated IMVs by negative-staining EM and on thin sections after preembedding labeling

Treatment	Gold particles/virion	
	Total no. (n = 50 particles)	% of total[a]
Negative staining		
Untreated	13.3	100
DTT treated	22.3	170
Preembedding labeling (in thin sections)	11.7	nd

[a] The values for untreated virions were normalized to 100%.

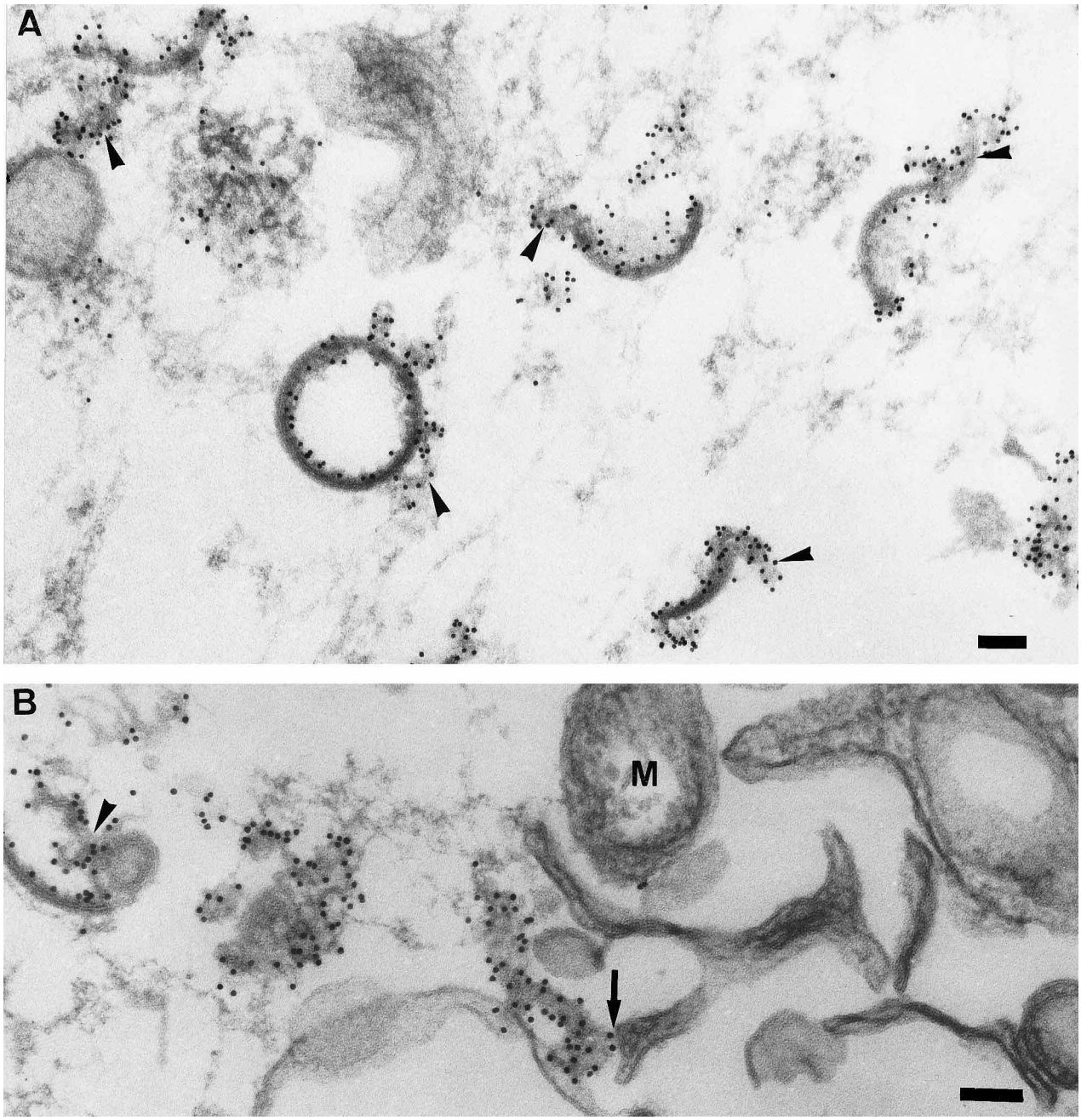

FIG. 15. Preembedding labeling for p16, Epon sections. In panel A almost all the label is associated with the inner membrane of the crescents. There is also strong labeling of membrane fragments in continuity with the crescents (arrowheads); one of these is also indicated in panel B. The arrow in panel B shows a strongly labeled membrane domain that is probably attached to the (unlabeled) ER. M, mitochondrion. Bars, 100 nm.

tosolic. Although membrane proteins with a single hydrophobic domain at their NH_2 terminus generally translocate the C terminus into the ER lumen, thereby adopting a so-called type II membrane topology (for a review see reference 31) p8 seems to be one of the few exceptions to this rule. Inspection of the p8 sequence shows that in fact its extreme NH_2 terminus is entirely hydrophobic and that the putative (α-helical) transmembrane domain is not preceded by a short stretch of more-hydrophilic amino acids, as is generally the case for type II membrane proteins (25, 31). This latter observation could possibly explain its unusual membrane topology.

From its sequence, p16 could be expected to span the membrane twice, having its NH_2 and C termini either lumenal or cytoplasmic. While protease digestion on in vitro-translated and -translocated p16 gave uninterpretable results, p16 was partially protected against proteolysis in vivo. The apparent protease resistance of p16 in infected cells can be explained in two possible ways. Either the protein folds into a protease-resistant structure, or it is shielded by other proteins. While protease digestion experiments gave no indication about the topology of p16, our indirect immunofluorescence data using SLO-permeabilized infected cells showed that the protein ex-

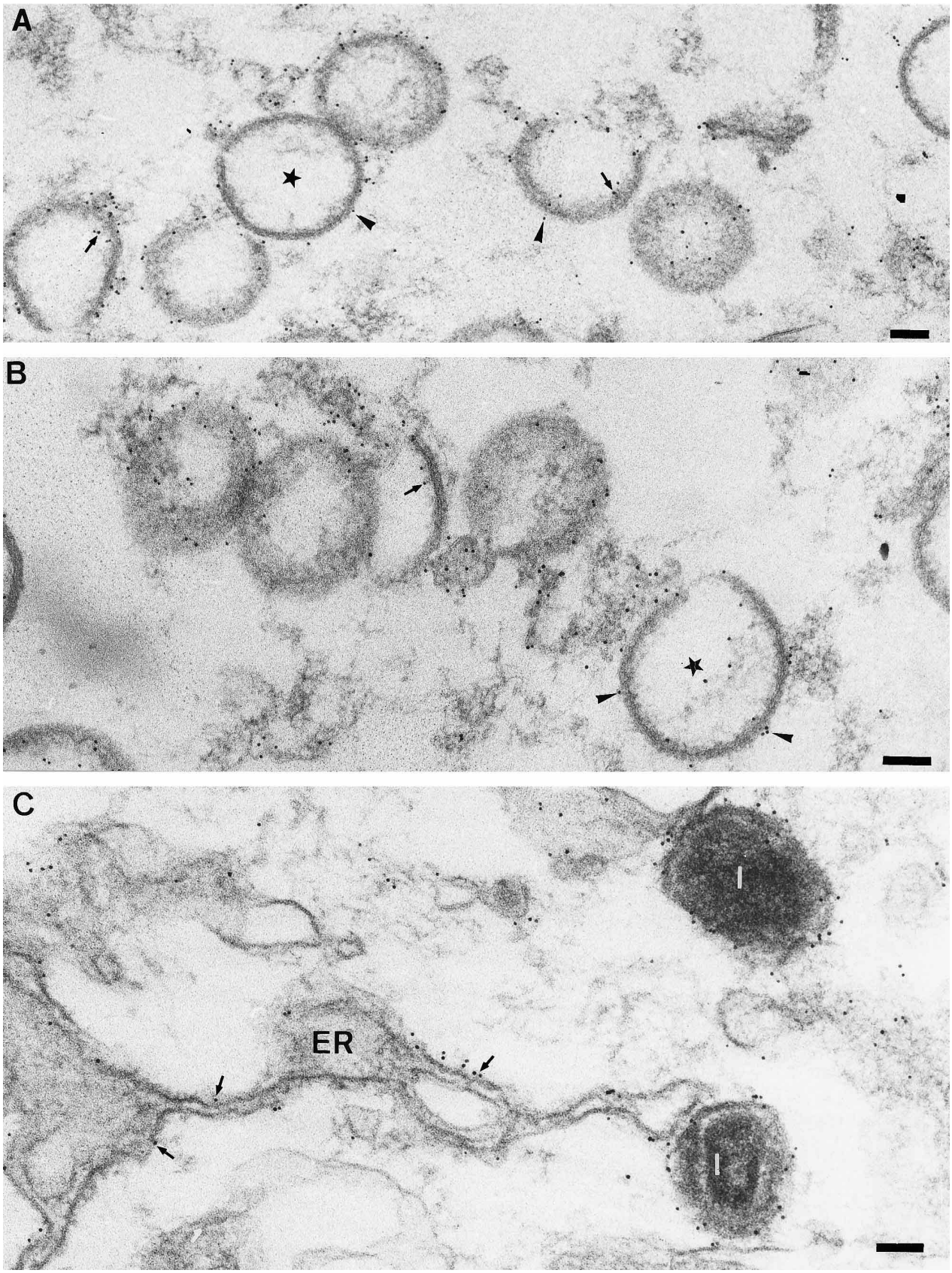

FIG. 16. Preembedding labeling for p8. (A and B) Crescents and IVs (stars). The arrows show labeling on the inner aspect, whereas the arrowheads indicate labeling on the outer aspect of these structures. Note that there is much more labeling on the outer side than is seen on cryosections (compare with Fig. 6). (C) Extensive labeling of the outside of IMVs (I); again, this is significantly more than that seen on cryosections (compare Fig. 5C and 7B). There is also significant labeling of the ER (arrows). Bars, 100 nm.

TABLE 2. Quantitation of preembedding labeling[a]

Location of gold particles	Total no. $n = 50$ IVs		% of total	
	p16	p8	p16	p8
Inside	370	66	95	30
Outside	20	157	5	70

[a] Gold particles (within 20 nm of the membranes) were counted that labeled either the inner or outer aspect of the IV membranes.

poses (at least partially) its C terminus toward the cytoplasm. More recent observations, however, suggest that p16 can adopt two topologies, both in vitro as well as in vivo (23a). Preliminary evidence, for instance, shows that a fraction of p16, both in vitro as well as in vivo, acquires N-linked glycans on its C terminus. This observation also explains why in vitro-translated and -translocated p16 migrates slower than its untranslocated counterpart (Fig. 9). How much of each topology is present under any one condition, as well as the significance of p16 adopting two different membrane associations, is currently being investigated.

Our results clearly show that p16 is a member of the inner of the two IV membranes. This was evident from labeling on cryosections as well as from the preembedding labeling EM studies, whereby the antibody clearly marked the inner aspect of the IVs. Moreover, these data were in full agreement with the protease digestions on intact IMV showing that the protein was fully protected as well as with the absence of labeling of the surface of the IMVs by negative staining EM. However, after DTT treatment a small fraction of the IMVs showed significant labeling for this protein. This can be attributed to the at least partial uncoating of the IMV that is seen with this treatment (see below).

In contrast to p16, the attribution of p8 to either of the two IV membranes was not unequivocal. Biochemical experiments suggested that p8 was entirely exposed to proteases on the surface of the IMV, a result that was in agreement with significant labeling (on the average of 13 gold particles per virion) on the surface of the IMV by negative-staining EM. However, as we have shown previously (28), the use of protease digestions with intact IMVs must be taken with extreme caution since, above a certain threshold, proteases gain access to proteins in internal virion locations. However, the notion that a substantial amount of p8 was indeed exposed on the outside of the IMV was also supported by the results of the preembedding labeling that showed substantial labeling of the IMV surface as well as the outer of the two IV membranes. In contrast, on cryosections the outer membrane of the IVs as well as of the IMVs labeled poorly, if at all, with the anti-p8 antibodies. This difference might be due to the masking of p8 on the outer surface, perhaps by a peripherally exposed protein. Since the preembedding labeling involves a water-lysis step, this putative masking factor(s) may be removed under hypotonic conditions. The significant increase of p8 labeling after treating IMVs with DTT seen by negative-staining EM could have two possible explanations. First, as for p16 the increase in labeling could be due to an uncoating of the IMV, exposing more of the inner membrane pool of p8 to its antibody. Second, it is also conceivable that reduction of a surface component would give more access to p8.

The preembedding labeling data showed that 30% of the labeling for p8 is found on the inner membrane of the crescent and the IV. On cryosections, essentially all the labeling is found on the inner side of these structures. Collectively, our data show that p8 is the first membrane protein which is enriched in both the inner and outer membrane of the IMV.

In conclusion, we have now characterized three important members of the IMV membranes, namely p21 (23) and in this study p16 and p8. Our data show that p16 is in the inner membrane together with the gene product of A17L, p21, which is also an abundant membrane protein of the IMV (23). In contrast, p8 was found both on the outer and inner membrane layers. Since all three proteins insert into the RER membrane before reaching their final destination, we envision that all three may play an important role in creating the virally modified microdomains of the ER/IC membrane which leads to the generation of the polarized two-membrane domains of the IV and the IMV.

ACKNOWLEDGMENT

J.K.L. was supported by a fellowship from Human Frontier Science Program Organization.

REFERENCES

1. **Blasco, R., and B. Moss.** 1991. Extracellular vaccinia virus formation and cell-to-cell virus transmission are prevented by a deletion of the gene encoding the 37,000-dalton outer envelope protein. J. Virol. **65:**5910–5920.
2. **Cairns, H. J. F.** 1960. The initiation of vaccinia infection. Virology **11:**603–623.
3. **Cobbold, C., J. T. Whittle, and T. Wileman.** 1996. Involvement of the endoplasmic reticulum in the assembly and envelopment of African swine fever virus. J. Virol. **70:**8382–8390.
4. **Cudmore, S., P. Cossart, G. Griffiths, and M. Way.** 1995. Actin-based motility of vaccinia virus. Nature **378:**636–638.
5. **Cudmore, S., R. Blasco, R. Vincentelli, M. Esteban, B. Sodeik, G. Griffiths, and J. Krijnse Locker.** 1996. A vaccinia virus core protein, p38, is membrane associated. J. Virol. **70:**6909–6921.
6. **Dales, S., and B. G. T. Pogo.** 1981. Biology of poxviruses. Virology monographs. Springer Verlag, Vienna, Austria.
7. **Dales, S., and E. H. Mosbach.** 1968. Vaccinia as a model for membrane biogenesis. Virology **35:**564–583.
8. **Ericsson, M., S. Cudmore, S. Shuman, R. C. Condit, G. Griffiths, and J. Krijnse Locker.** 1995. Characterization of *ts*16, a temperature-sensitive mutant of vaccinia virus. J. Virol. **69:**7072–7086.
9. **Essani, K., and S. Dales.** 1979. Biogenesis of vaccinia: evidence for more than 100 polypeptides in the virion. Virology **95:**385–394.
10. **Goebel, S. J., G. P. Johnson, M. E. Perkus, S. W. Davis, J. P. Winslow, and E. Paoletti.** 1990. The complete DNA sequence of vaccinia virus. Virology **179:**247–266.
11. **Griffiths, G.** 1993. Fine structure immunocytochemistry. Springer Verlag, Heidelberg, Germany.
12. **Griffiths, G., R. Pepperkok, J. Krijnse Locker, and T. E. Kreis.** 1995. Immunocytochemical localization of beta-COP to the ER-Golgi boundary and the TGN. J. Cell Sci. **108:**2839–2856.
13. **Griffiths, G.** 1996. On vesicle and membrane compartments. Protoplasma **195:**37–58.
14. **Griffiths, G., M. Ericsson, J. Krijnse Locker, T. Nilsson, H. D. Soeling, B. L. Tang, S. H. Wong, and W. Hong.** 1994. Ultrastructural localization of the mammalian KDEL receptor in cultured cells and tissues. J. Cell Biol. **127:**1557–1574.
15. **Grimley, P. M., E. N. Rosenblum, S. J. Mims, and B. Moss.** 1970. Interruption by rifampicin of an early stage in vaccinia virus morphogenesis: accumulation of membranes which are precursors of virus envelopes. J. Virol. **6:**651–659.
16. **Hammond, C., and A. Helenius.** 1994. Quality control in the secretory pathway: retention of a misfolded viral membrane glycoprotein involves recycling between the ER, intermediate compartment and the Golgi apparatus. J. Cell Biol. **126–41–52.**
17. **Hiller, G., and K. Weber.** 1985. Golgi-derived membranes that contain an acylated viral polypeptide are used for vaccinia virus envelopment. J. Virol. **55:**651–659.
18. **Jensen, O. N., T. Houthaeve, A. Shevchenko, S. Cudmore, T. Ashford, M. Mann, G. Griffiths, and J. Krijnse Locker.** 1996. Identification of the major membrane and core proteins of vaccinia virus by two-dimensional electrophoresis. J. Virol. **70:**7485–7497.
19. **Johnson, G. P., S. J. Goebel, and E. Paoletti.** 1993. An update on the vaccinia virus sequence. Virology **196:**381–401.
20. **Krijnse Locker, J., M. Ericsson, P. J. M. Rottier, and G. Griffiths.** 1994. Characterization of the budding compartment of mouse hepatitis virus: evidence that transport from the RER to the Golgi complex requires only one vesicular transport step. J. Cell Biol. **124:**55–70.

21. **Krijnse Locker, J., J. K. Rose, M. C. Horzinek, and P. J. M. Rottier.** 1992. Membrane assembly of the triple-scanning coronavirus M protein. Individual transmembrane domains show preferred orientation. J. Biol. Chem. **267:** 21911–21918.
22. **Krijnse Locker, J., R. G. Parton, S. D. Fuller, G. Griffiths, and C. G. Dotti.** 1995. The organization of the endoplasmic reticulum and the intermediate compartment in cultured rat hippocampal neurons. Mol. Biol. Cell **6:**1315–1332.
23. **Krijnse Locker, J., S. Schleich, D. Rodriguez, B. Goud, E. J. Snijder, and G. Griffiths.** 1996. The role of a 21-kDa viral membrane protein in the assembly of vaccinia virus from the intermediate compartment. J. Biol. Chem. **271:** 14950–14958.
23a. **Krijnse Locker, J., et al.** Unpublished data.
24. **Moss, B., E. N. Rosenblum, E. Katz, and P. M. Grimley.** 1969. Rifampicin: a specific inhibitor of vaccinia virus assembly. Nature **224:**1280–1284.
25. **Rapoport, T. A.** 1985. Protein translocation across and integration into membranes. Crit. Rev. Biochem. **20:**73–137.
26. **Rodriguez, D., M. Esteban, and J. R. Rodriguez.** 1995. Vaccinia virus A17L gene product is essential for an early step in virion morphogenesis. J. Virol. **69:**4640–4648.
27. **Rodriguez, J. R., C. Risco, J. L. Carrascosa, M. Esteban, and D. Rodriguez.** 1997. Characterization of early stages in vaccinia virus membrane biogenesis: implication of the 21-kDa and a newly identified 15-kDa envelope protein. J. Virol. **71:**1821–1833.
28. **Roos, N., M. Cyrklaff, S. Cudmore, R. Blasco, J. Krijnse Locker, and G. Griffiths.** 1996. A novel immunogold cryoelectron microscopic approach to investigate the structure of the intracellular and extracellular forms of vaccinia virus. EMBO J. **15:**2343–2355.
29. **Saraste, J., U. Lahtinen, and B. Goud.** 1995. Localization of the small GTP-binding protein rab1p to early compartments of the secretory pathway. J. Cell Sci. **108:**1541–1552.
30. **Schmelz, M., B. Sodeik, M. Ericsson, E. Wolffe, H. Shida, G. Hiller, and G. Griffiths.** 1994. Assembly of vaccinia virus: the second wrapping cisterna is derived from the trans Golgi network. J. Virol. **68:**130–147.
31. **Singer, S. J.** 1990. The structure and insertion of integral proteins in membranes. Annu. Rev. Cell Biol. **6:**247–296.
32. **Slot, J. W., H. J. Geuze, S. Gigengack, G. E. Lienhard, and D. E. James.** 1991. Immuno-localization of the insulin regulatable glucose transporter in brown adipose tissue of the rate. J. Cell Biol. **113:**123–135.
33. **Sodeik, B., G. Griffiths, M. Ericsson, B. Moss, and R. W. Doms.** 1994. Assembly of vaccinia virus: effects of rifampin on the intracellular distribution of viral protein p65. J. Virol. **68:**1103–1114.
34. **Sodeik, B., R. W. Doms, M. Ericsson, G. Hiller, C. E. Machamer, W. van't Hof, G. van Meer, B. Moss, and G. Griffiths.** 1993. Assembly of vaccinia virus: role of the intermediate compartment between the endoplasmic reticulum and the Golgi stacks. J. Cell Biol. **121:**521–541.
35. **Sodeik, B., S. Cudmore, M. Ericsson, M. Esteban, E. G. Niles, and G. Griffiths.** 1995. Incorporation of p14 and p32 into the membrane of the intracellular mature virus. J. Virol. **69:**3560–3574.
36. **Takahashi, T., M. Oie, and Y. Ichihashi.** 1994. N-terminal amino acid sequences of vaccinia virus structural proteins. Virology **202:**844–852.
37. **Wolffe, E. J., D. M. Moore, P. J. Peers, and B. Moss.** 1996. Vaccinia virus A17L open reading frame encodes an essential component of nascent viral membranes that is required to initiate morphogenesis. J. Virol. **70:**2797–2808.